

We E106 01

Parametrization for 2-D SH Full Waveform Inversion

P. Bharadwaj* (Delft University of Technology), W.A. Mulder (Shell GSI BV & Delft University of Technology) & G.G. Drijkoningen (Delft University of Technology)

SUMMARY

With single-parameter full waveform inversion, estimating the inverse of the Hessian matrix will accelerate the convergence, but is computationally expensive. Therefore, an approximate Hessian, which is easier to compute, is often used. Similarly, in the case of multi-parameter full waveform inversion, the computation of the Hessian terms that contain derivatives with respect to more than one type of parameter, called cross-parameter Hessian terms, is not usually feasible. If the nonlinear inverse problem is well-posed, then the result should be independent of the parametrization choice provided we start close to the global minimum. However, the choice of parametrization will affect the rate of convergence to the exact solution and the “best” choice of parametrization is the one with the fastest rate. If the inverse problem is ill-posed the choice of parametrization introduces a bias towards a particular solution among the non-unique ones that explain the data. This obfuscates the search for the “best” parametrization. We investigated parametrization choices for a 2-D SH experiment where only the reflected wavefield is recorded. Our numerical examples suggest that certain type of scatterers are better inverted by one parametrization choice than another due to the parametrization bias. Therefore, there is nothing like a “best” parametrization in these single-component SH examples.

Introduction

Quantitative imaging of various near-surface elastic parameters is essential for many civil engineering applications. This may be achieved by full waveform inversion (FWI) of the recorded elastic wavefield (Tarantola, 1986; Virieux and Operto, 2009), which is sensitive to the shear and compressional properties of the weathered layers. FWI is a nonlinear data fitting procedure that minimizes the least square misfit between the recorded and modelled seismic data to estimate the subsurface parameters. Given the size of the problem, it is only feasible in practice to use descent methods for optimization. Ideally, the gradient needs to be conditioned by the inverse of the Hessian matrix to reduce the number of iterations needed to reach an acceptable solution (Pratt et al., 1998). Because this is computationally expensive, an approximate Hessian is often used as preconditioning matrix. Alternatively, or in combination, a BFGS-type of optimization method that estimates the inverse Hessian from subsequent iterations can be applied. In the case of multi-parameter full waveform inversion, the computation of the Hessian terms that contain derivatives with respect to more than type of parameter, called cross-parameter Hessian terms, is not usually feasible at each iteration. If a simple gradient-based minimization with, for instance, just scalar weights for each of the parameter types is used, different choices for parametrization can be interpreted as different preconditioners, i.e., different approximations of the block-diagonal of the inverse Hessian. This will affect the convergence rate. Intuitively, if the diagonal blocks, capturing all model parameters in a single subsurface location, have small cross-parameter terms, they are better decoupled during inversion and this will help convergence (Tarantola, 1986; Operto et al., 2013). The obvious question is: which choice of parameters provides the fastest convergence?

Aside from the notorious cycle skipping in FWI that causes convergence to the nearest local minimum, there is another problem: the solution of the nonlinear inverse problem is likely to be non-unique. If one ignores the non-uniqueness due to the absence of high frequencies, there is always the imprint of a finite acquisition geometry. In the presence of non-uniqueness, a different choice of parametrization may lead to a different inversion result that provide the same synthetic data at convergence. This is similar to null-space components in linear inverse problems. Therefore, a particular parameter choice implies a bias towards one type of solution over another. As a result, the search for the “best” parametrization is likely to be obfuscated by non-uniqueness problems. In the following, we will examine the choice of parametrization in case of a 2-D SH experiment used for near-surface ground characterization.

Parametrization for 2-D SH waveform inversion

Inversion for various subsurface parameters using the seismic data will reduce the risk of collapses during underground tunnel construction. In the near surface, shear properties can often be imaged better and with higher resolution compared to P-wave properties. Hence, in order to facilitate ground prediction ahead of a tunnel boring machine (TBM), active surveys with shear-wave vibrators are carried out especially while boring in soft soils. In such surveys, a few shear-wave vibrators are placed in front of the cutting wheel and they primarily inject a force in the direction perpendicular to the drilling path. Particle velocity in this direction is measured using inline receivers, typically around 10. As a simplified but useful model, we can consider 2-D SH waves in the (x, z) -plane, with a force in the y -direction. In order to invert such a dataset, we parametrize the Earth model by two sets of parameters, namely density, ρ , and shear-wave speed, V_s , or their combinations, for instance, with shear impedance, $I_s = \rho V_s$, or one of the Lamé parameters, $\mu = \rho V_s^2$. The SH wavefield is not sensitive to the compressional properties of the subsurface and its propagation obeys the 2-D wave equation, $\mathbf{L}u_y - f = 0$, with $\mathbf{L} = \rho \frac{\partial^2}{\partial t^2} - \nabla \cdot \rho V_s^2 \nabla$. Here, u_y denotes the out-of-the-plane particle velocity component, $\nabla = (\frac{\partial}{\partial x}, \frac{\partial}{\partial z})^T$ and f is the source term. Next, we analyze the effect of different parametrizations on the inversion results using two synthetic test models. We placed 33 evenly spaced receivers at $x = 1$ m starting from $z = 2$ m to $z = 16$ m. Synthetic data were generated in both cases for 9 sources, 2 m apart as shown in the V_s model of Figure 1a. A time-domain staggered-grid finite-difference code for the SH wave equation was used to model the data and to perform the adjoint wavefield computations required for the gradients (Fichtner, 2010). The optimization was performed by a preconditioned conjugate-gradient method. During the inversion,

the source wavelet is assumed to be known and the direct arrivals are muted from the data. In all these experiments, we also assume that low-frequency source signals, typically 5–10Hz in this setting, can be reliably recorded. This will avoid the notorious cycle-skipping problem.

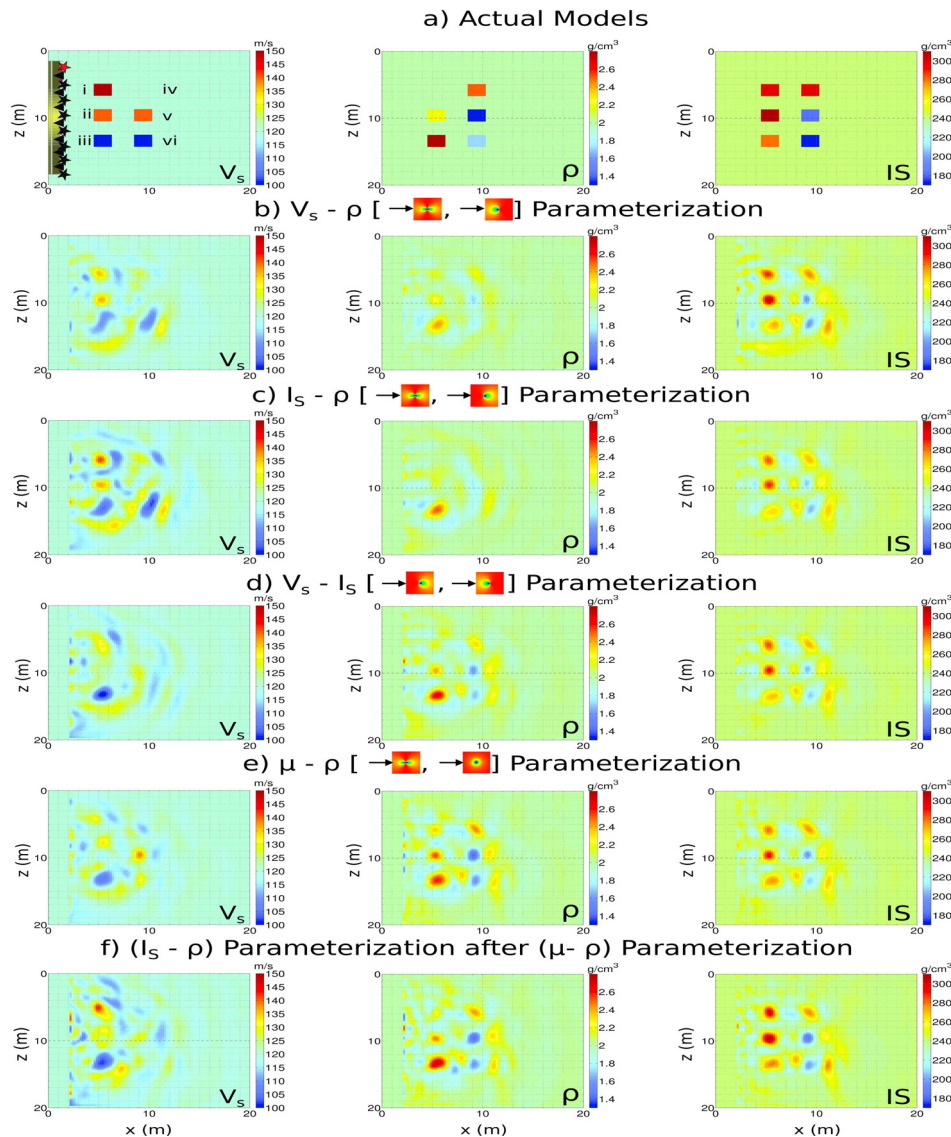


Figure 1 A model with six blocky perturbations that have different radiation patterns. (a). The actual V_s , ρ and I_s models are plotted. (b). Multi-parameter full waveform inversion results after 30 iterations using the (V_s, ρ) -parameterization. (c). As (b) but with a (I_s, ρ) -parameterization, (d) with (V_s, I_s) , (e) with (μ, ρ) . (f). Inversion results with a (I_s, ρ) -parameterization after 40 iterations using initial models plotted in (e). The radiation pattern of the scattered wavefield due to perturbation in each parameter class is also plotted where the the primary wavefield is incident from the direction marked by the black arrow.

Six-block model: Figure 1a depicts an assumed Earth model with six blocky scatterers, marked (i)–(vi). The velocity and density anomalies (Table 1) are such that they have different radiation patterns. The Ricker source wavelet has a peak frequency of 14Hz and full-bandwidth inversion with different parameterizations is carried out with a maximum of 30 iterations after which the convergence slows down. We started from the same initial homogeneous model of $V_s = 120\text{m/s}$ and $\rho = 2\text{g/cm}^3$. Figure 1b shows the inversion results for a (V_s, ρ) -parameterization. Note that, in this case, the inversion tries to explain the radiation patterns of different model blocks by linearly combining the radiation patterns due to V_s

Table 1 Inversion results of the model with six blocks.

Block No.	V_s Anomaly (m/s)	ρ Anomaly (g/cm ³)	I_s Anomaly	Recommended parametrization
i	+30	0	positive	$(V_s, \rho), (I_s, \rho)$
ii	+20	+0.2	positive	$(V_s, \rho), (I_s, \rho)$
iii	-20	+0.8	positive	$(V_s, I_s), (\mu, \rho)$
iv	0	+0.5	positive	$(V_s, I_s), (\mu, \rho)$
v	+20	-0.7	negative	(μ, ρ)
vi	-20	-0.3	negative	$(V_s, \rho), (I_s, \rho)$

and ρ perturbations, plotted in Figure 1b for normal incidence.

Since the blocks have different radiation patterns, it is possible that the inversion is more successful (at least in the first few iterations) in explaining the radiation pattern due to one particular block than another. Here we observe that the block (i) of the model is best inverted using either a (V_s, ρ) - or (I_s, ρ) -parametrization, compared to other parametrization choices. Similarly, block (iv) is best recovered using either a (μ, ρ) - or (V_s, I_s) -parametrization. Table 1 lists suitable parametrizations for each of the blocks. Notice that the inverted I_s models in all cases (Figures 1b–1e) are similar, which means that the zero-offset data are well explained in each case. We observe that if the radiation pattern of a scatterer has a larger velocity anomaly than density anomaly, as in blocks (i), (ii) and (vi), it is more easily recovered with a (V_s, ρ) -parametrization. Otherwise, if it has a larger density anomaly, as in blocks (iii), (iv) and (v), it is quicker recovered with a (μ, ρ) -parametrization.

This could be due to the potential presence of non-uniqueness in the current inverse problem, causing different choices for the parametrization to produce different results, similar to the null-space problem encountered in linear inverse problems such as, for instance, least-squares migration. The following observations suggest that our inverse problem be non-unique:

1. The inversion did not converge to a band-limited version of the true solution even when we carried out hundreds of conjugate-gradient iterations using various parametrizations.
2. We used the resultant model from the (μ, ρ) -parametrization in Figure 1e as an input to (I_s, ρ) -parameter inversion. After 40 iterations, there is no noticeable change in the model, plotted in Figure 1f, which suggests non-uniqueness.
3. The (V_s, ρ) -parametrization inversion was unsuccessful in recovering blocks (iv) and (v) even with a much denser acquisition that also included large offsets.

Given these observations as well as the data and model residual plots in Figure 2, it appears we cannot decide on the “best” parametrization for this experiment.

Karst model: A Karst model is plotted in Figure 3. The source wavelet is a band-limited delta function (5–60Hz). We applied multi-scale FWI by first inverting the data between 5 and 10Hz, followed by nine subsequent 5-Hz bands up to 60Hz. In this case, the anomalies are such that they fall under the category of block (ii) of the previous model. Hence, we expect them to be better recovered by using a (V_s, ρ) -parametrization. This is evident from the inversion results shown in Figure 3.

Conclusions

We analysed different parametrizations for the case of a 2-D SH seismic experiment, carried out to facilitate tunnel boring. Synthetic results demonstrate that a particular choice of parametrization is effective in reconstructing a certain type of anomaly in the subsurface. We conclude that there is nothing like the “best” parametrization choice in our single-component SH examples, but the choice of shear velocity and density gave the cleanest results for our synthetic model.

Acknowledgements

This work was carried out as part of the NeTTUN project. The first author thanks Jan Thorbecke (<http://janth.home.xs4all.nl/>) for helpful discussions on numerical wave-equation modelling.

References

- Fichtner, A. [2010] *Full seismic waveform modelling and inversion*. Springer.
- Operto, S. et al. [2013] A guided tour of multiparameter full-waveform inversion with multicomponent data: From theory to practice. *The Leading Edge*, **32**(9), 1040–1054.
- Pratt, R.G., Shin, C. and Hicks, G. [1998] Gauss-Newton and full Newton methods in frequency-space seismic waveform inversion. *Geophysical Journal International*, **133**(2), 341–362, doi:10.1046/j.1365-246X.1998.00498.x.
- Tarantola, A. [1986] A strategy for nonlinear elastic inversion of seismic reflection data. *Geophysics*, **51**, 1893–1903.
- Virieux, J. and Operto, S. [2009] An overview of full-waveform inversion in exploration geophysics. *Geophysics*, **74**(6), WCC1–WCC26, doi:10.1190/1.3238367.

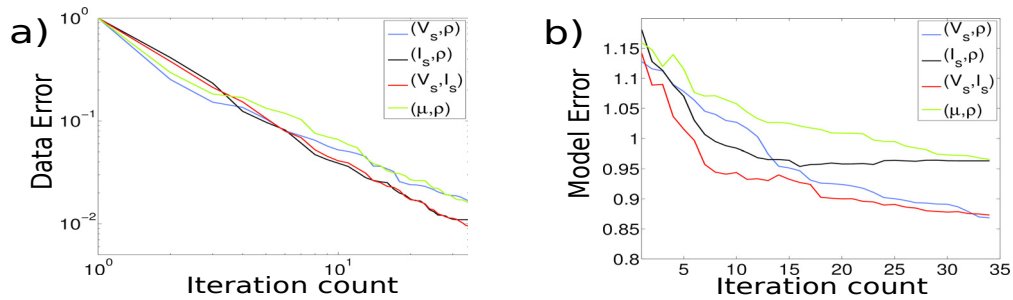


Figure 2 Six-block model inversion: (a) data error and (b) model error vs. iteration count. Since the reconstruction is band-limited, there will always be a $O(1)$ model error.

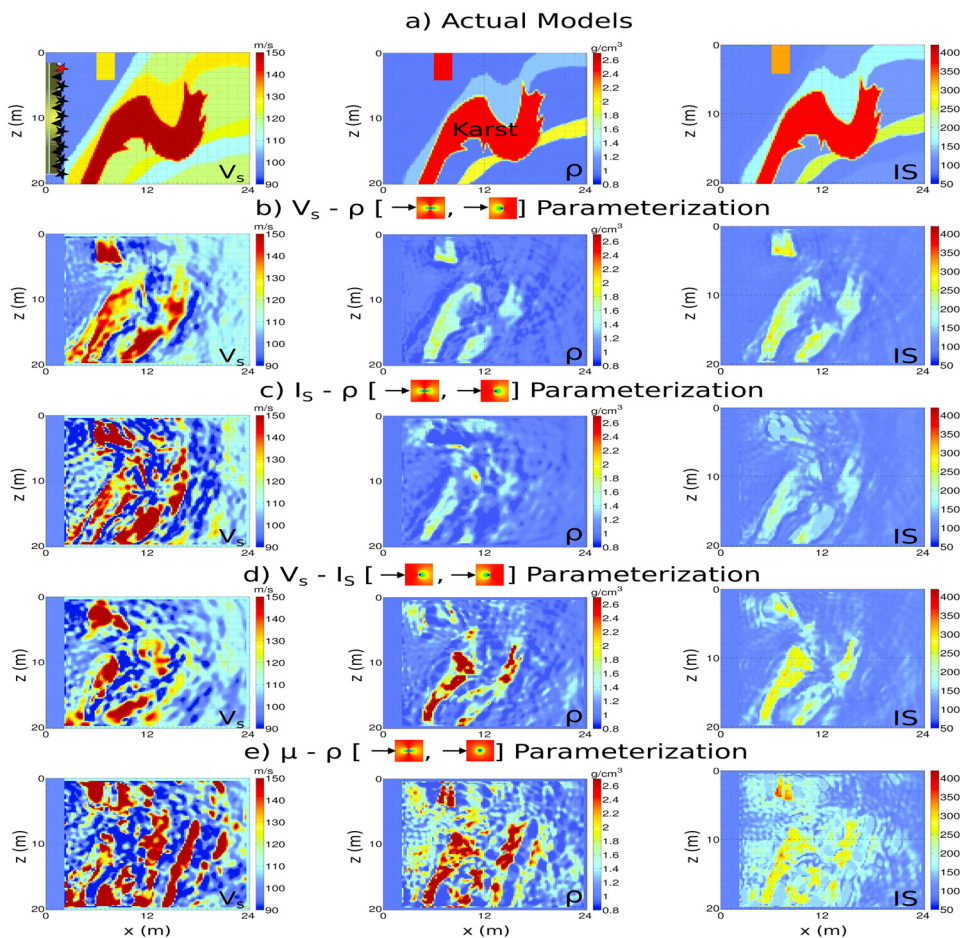


Figure 3 Inversion results for the Karst model, similar to Figures 1a–1e, after 200 iterations.